JJMIE

Volume 20, Number 1, March. 2026
ISSN 1995-6665
Pages 17– 27
https://doi.org/10.59038/jjmie/200102
Editor-in-Chief: Prof. Faris M. AL-Oqla

Jordan Journal of Mechanical and Industrial Engineering

Computational and Experimental Study of Velocity Anisotropy and Slurry Hydrodynamics in Wafer-Pad CMP: Rs-Governed Material Removal with Machine Learning Prediction

Abdullah Hasni, Syed Muhammad Raza, Hannan Ahmed Siddiqui,

Mumtaz Hussain Qureshi

Department of Mechanical Engineering, NED University of Engineering & Technology, Karachi, Pakistan

Received 25 Jun 2025 *Accepted 1 Feb 2026*

Abstract

Chemical Mechanical Polishing (CMP) remains a critical challenge in advanced semiconductor manufacturing, particularly for leading chip producers such as NVIDIA and TSMC, where sub-5 nm architectures, HBM stacking, and chiplet integration demand exceptionally tight planarity control. The failure of traditional CMP models based on Preston's equation to account for nonlinear slurry–pad–wafer interactions, velocity anisotropy, and pad wear variability results in defects such dishing, erosion, and non-uniform thinning. To get beyond these restrictions, this work offers a unique kinematic–computational–machine learning (ML) framework. Analysis of the slurry-flow behavior and velocity distribution over a 100 mm wafer at various RPM ratios shows that Rs = 1.0 minimizes velocity non-uniformity, whereas Rs > 1 increases MRR and Rs < 1 decreases it. High-accuracy MRR prediction is produced by a Random Forest model with LOOCV, and the Pad–Wafer RPM Ratio is found to be the primary optimization variable. Additionally, a new sweeping-rotation technique is presented to maintain planarization and enhance shear distribution. The suggested methodology directly addresses the CMP limitations encountered by next-generation GPU and semiconductor production by enabling AI-driven CMP optimization, which offers greater uniformity, decreased defectivity, and increased yield.

Keywords: Chemical Mechanical Polishing (CMP), Velocity Anisotropy, Material Removal Rate (MRR), Pad–Wafer RPM Ratio, Machine Learning Based Process Optimization.

1. Introduction

CMP is a critical technique for achieving planar surfaces in semiconductor fabrication. It combines mechanical abrasion and chemical reactions to remove film layers and enhance wafer uniformity. However, the interplay of slurry flow, relative velocity, and material removal rate remains complex and requires further investigation. Previous studies have examined CMP kinematics, pressure distribution, and slurry transport, but gaps exist in accurately predicting MRR under varying process conditions. Traditional models, such as the Preston equation, assume a linear relationship between MRR and process variables, but fail to capture nonlinear interactions. Recent advancements in AI and machine learning provide an opportunity to refine MRR predictions and optimize CMP processes. Furthermore, we introduce a novel sweeping-rotation concept, which enhances polishing efficiency beyond conventional fixed-speed approaches. The findings reinforce the expected impact of velocity variation on MRR and demonstrate the potential of AI-driven process optimization in wafer CMP, bridging the gap between theoretical models and practical enhancements in polishing uniformity and efficiency. A mix of mechanical polishing and a chemical reaction to remove small pieces of film that have been deposited on a wafer, leaving the surface smoother and more uniform. The high resistance and electromigration issues of metal lines brought on by sidewall thinning linked to inadequate step coverage of metal PVD processes are resolved by a planarized surface. Additionally, the need for prolonged exposure and development to remove the thicker photo resist regions caused by dielectric stages has been removed by a planarized surface. In order to achieve a smooth and uniform surface, improve layer stacking, and improve electrical characteristics in semiconductor devices, CMP (Chemical Mechanical Planarization) techniques are widely used in the fabrication of IC chips. In shallow trench isolation (STI), an integrated circuit feature that stops electric current from leaking between nearby semiconductor device components, they are utilized to eliminate bulk oxide deposit. A polishing pad, a slurry dispenser unit, and a spinning wafer carrier which presses the wafer face down against the polishing pad make up a CMP system.

* Corresponding author e-mail: hasniabdullah975@gmail.com.

In the IC sector, CMP procedures employ water-based polishing slurries that contain chemical additives and abrasive particles [1]. The wafer is placed face down against the polishing pad after the slurry has been poured over its surface. Typically, the wafer carrier and platen rotate in the same direction. Material is removed from the wafer surface by the combined action of chemical etching and mechanical abrasion. Protruding areas receive more mechanical abrasion and are removed faster than recessed areas, this helps planarized the wafer surface. Protruding areas receive more mechanical abrasion and are removed faster than recessed areas, this helps planarized the wafer surface [2-3].

Investigations for the flow between a wafer and pad during CMP processes, which consolidated the numerical and experimental work. The numerical approach has anticipated the pressure and velocity below the wafer whereas the experimental approach is predicted the fluid film thickness and slurry flow beneath the wafer. The result shows the significant difference between the Embossed Politex pad and the IC1000 pad. The IC1000 pad represented a gradient in the slurry flow only in the inner third of the wafer whereas the remaining part of the wafer containing a relatively constant slurry age. The Embossed Politex pad represented the linear gradient across the wafer. The Politex pad absorbed the fluid inside the macro-structure of the pad due to which fluid is not mixed well throughout the pad surface. But opposite behavior is observed in the IC1000 pad because the microstructure of the pad is not effectively trapped the fluid and the slurry gradient are smoothed and reduced below the wafer. In IC1000 pad, the conditioning process is not produced the large disturbance in mixing characteristics [4-5].Kinematics in the CMP technique is examined in order to test for relative velocity non-uniformity. The reason for the decreased velocity non-uniformity is the great distance between the wafer and pad centers. Particle aggregation and abrasion efficiency degradation are caused by long pad travel, as seen by a saturation of removal rate at high velocity. The Preston equation is insufficient to illustrate the polish rate as a function of velocity. However, the abrasive degradation performance which is dependent on the velocity or rate of material removal, is consolidated using the modified Preston equation. The usefulness of two models remained neutral with edge effect [6]. Kinematic analysis in the CMP process is affected by the velocity uniformity, sliding-distance distribution, sliding distance uniformity, velocity distribution size and shape, and friction force direction. The non-dimensional parameter xi is used to characterize each of these parameters. Velocity and sliding distance uniformity It is shown that the value xi has little effect on the sliding distance uniformity of the wafer, but it significantly affects the velocity-distribution uniformity. Head rotation speed has a slight impact on the rate of material removal when pad speed is constant, but it has a big impact when pad speed varies. To reduce the gradient homogeneity, it is proposed that low pressure conditions on the wafer or pad are possible [7-8]. The kinematic relationship between the polishing pad and the wafer with friction properties is examined in this study. Thewafer/pad friction characteristics are developed using the Lu Gredynamic friction model. Relationships between polishing settings, spindle and roller moments, and wafer/pad friction coefficients are suggested. In contrast to m>0, the impacts of pad conditioning and patterned wafer resulted in substantial nonuniformity. Further, for the polishing pad the large $R^{c/d}$ is produced at two different limits of the ratio [9].This research relates with investigation of the material removal rate (MRR)approach in the fast-polishing process and renew and justified the MRR equation. The results show that the MRR is high by adjusting the properties of slurry and pad. MRR is produced the significant effect on the within-wafer nonuniformity (WIW-NU)because of the downpressure distribution [10-11]. The Particle Image Velocimetry (PIV) algorithm is used to describe the slurry flow during polishing in order to better understand material removal during the CMP process [12]. The primary benefit of using the PIV technique is that it draws attention to the intricate details of the slurry movement. The novel multi-physics model, which is based on wear theory, fluid mechanics, contact mechanics, and chemical reaction kinetics, is investigated. The impacts of fluid movement, chemical reactions, and mechanical abrasion on the removal rate are illustrated using the Multiphysics model. Chemical reaction kinetics model is proposed to determine a relationship between the removal rate and slurry components and chemical reaction constants. The concentrations of chemical reagents are then computed through solving convective diffusive mass transport equation, average Reynolds equation and slurry velocity distributions [13]. During chemical mechanical planarization, data on pad-wafer shear force and normal force are measured. The findings indicate that the force data provides insight into the mean solid contact and fluid pressures at the interface and describes the wafer perspective in comparison to the pad. Modeled the accurate analytic approximation to the solution of the Reynolds equation for the mean fluid pressure in the slurry layer during CMP [14]. The capillary effect is used to create a new slurry flow.

To investigate the capillary effect, a fiber array is positioned on the pad, and the slurry is evenly dispersed throughout the pad's diameter. According to observations, the suggested slurry delivery technique does not significantly alter the removal rate when using experimentally concentrically grooved pads. However, in contrast to the traditional slurry-nozzle supply system, orthogonal groove polishing pads with varying depths produce a high removal rate [15]. Examining how velocity distribution affects slurry flow over a100mm wafer during the CMP process is the aim of this work. Using the Preston equation as a basis, the simulation study shows how velocity variation affects the MRR. The first topic covered is the CMP kinematic structure, which is employed to assess the velocity distribution at the wafer-pad contact [16-17].The removal rate profiles with the rpm ratio pad/wafer settings71/59,71/61,71/67,71/71,71/73,and 71/79 are analyzed, and MRR is investigated in relation to polishing time. Lastly, the output of all the simulations was discussed and the conclusion was drawn.

2. Materials & Methods

The rotary mechanism, which is typically employed in solid-state manufacturing is the foundation of the CMP process. Achieving a uniform material removal rate throughout the entire wafer area is the primary purpose of the kinematic parameters in the CMP machine. Kinematic computations are predicated on the earlier research. Fig. 1. establishes several settings for this study and provides a schematic explanation of the rotating mechanism in the CMP process. The kinematic settings arebased on the parameters α, β, $\omega_W$and $\omega_P$represent the distancebetween pad and wafer centers, distance from the center to the given

point (P) on the wafer and angular velocity of wafer and pad, respectively. The relative velocity($V_{w/p}$) of the given point p on the wafer surface with respect to pad is expressed as:

$$\vec{V}_{w/p}=\vec{V}_w-\vec{V}_p \quad (1)$$

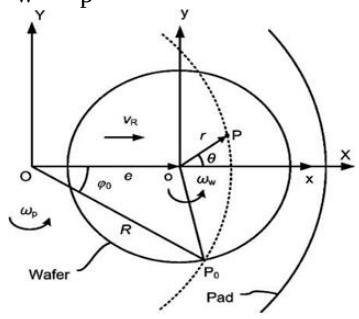

Figure 1.CMP parameters for kinematic analysis

where VP is pad velocity, and Vw is wafer velocity at that point.

The effect of oscillation is negligible. The relative velocity at any point on the wafer is constant when the pad and wafer rotate with the same speed. The relative velocity is transformed from the above equation into the relative velocity components Vx and Vy. The dimensionless parameters are the relative radius r and the non-dimensional variable μ are introduced to define the relative velocity with more predominantly.

$$V_x=\beta(\omega_p-\omega_w)\sin(\omega_w t)=\omega_p\alpha r\mu\sin\theta V_y=-\beta(\omega_p-\omega_w)\cos(\omega_w t)+\omega_p\alpha=-\omega_p\alpha(r\mu\cos\theta+1) \quad (2)$$

where $r=\frac{\beta}{\beta_w}$, $\mu=\frac{\beta_w}{\alpha}(1-R_s)$, rpm ratio $(R_{rpm})=\frac{\omega_w}{\omega_p}$, $\theta=\omega_w t$, and β_w represents wafer radius. From the all above parameters, μ is the most dominant parameter which is played a vital role in terms of kinematic conditions for CMP. In this study, μ is defined as a 'kinematic number' which is covered the explanation of the size effect of (β_w), the effect of the polishing table size (β: distance between rotation centers), and the rotation speed of each axis ($1-R_s$).

From equations (2) and (3) the relative velocity distribution between the wafer and pad can be expressed as

$$V_{w/p}=\sqrt{V_x^2+V_y^2}=\omega_p\alpha\sqrt{(r\mu)^2+2r\mu\cos\theta+1} \quad (3)$$

In this study, μ is less than 0.5 ($|\mu|\leq 0.5$) over the wide range of kinematic conditions because of the limitation of the CMP equipment (i.e.,$\beta_w/\alpha<1$ and $|1-R|<0.5$).

2.1. Velocity distribution between Wafer and Pad motion

Velocity distribution is a crucial component for the explanation of the slurry flow and material removal rate in the relative wafer and pad motion. The velocity distribution at the wafer/pad interface is depicted in Fig. 2. To test the velocity distribution at four distinct portions on the pad surface beneath the wafer region, as indicated in Table 1, the wafer and pad rotational rates are adjusted to 59 and 71 revolutions (rev) per minute (min).

According to Table. 1., normalized velocity profiles are addressed in Fig .3., which shows the slurry flow velocity variation at the wafer/pad interface along one revolution (0 to 360 degree) of the pad. Four regions are considered under the wafer and each region is the ratio between the distance from center to any point P on the wafer (r) to the radius of the wafer (R) that is r/R and the selected values are 0.25,0.5,0.75 and 1.0. The results show that at the wafer/pad interface, normalized velocity distribution ranges at region-1 of value 0.25 is from 0.375 to 0.625, at region-2 of value 0.5 is from 0.25 to 0.75, region-3 of value 0.75 is from 0.125 to 0.875 and region-4 of value 1 is from 0 to 1.

Observations show that low and high variations in the normalized relative velocity are obtained at near the center and edge of the wafer respectively and the other variations are intermediate between center to edge of the wafer. Hence, the range of the variations increases with the radius of wafer.

Table. 1. Wafer positions with respect to pad with R= 50 mm

Wafer/pad surface	Wafer center to point p (r)(mm)	r/R
Region-1-(near center of wafer, yellow vector plot))	12.5	0.25
Region-2-(intermediate location, green vector plot)	25	0.5
Region-3-(intermediate location, red vector plot)	37.5	0.75
Region-4-(edge of the wafer, orange vector plot)	50	1

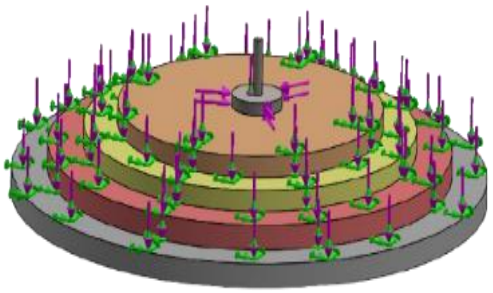

Figure 2. Velocity distribution for both wafer/pad motionwith wafer = 59 rev/min and pad = 71 rev/min. The numbers 1, 2, 3 and 4 are show the regions under the wafer in mm.

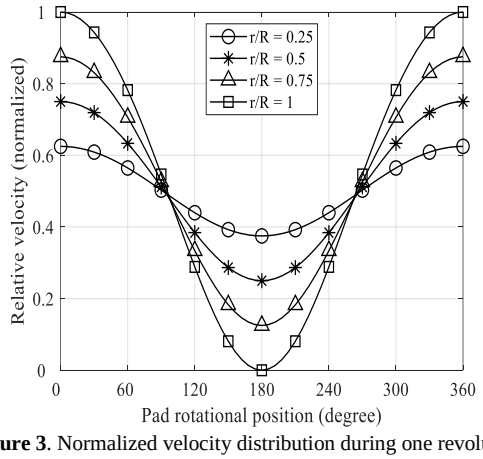

Figure 3. Normalized velocity distribution during one revolution of wafer/pad motion.

The rpm ratio of the wafer/pad =59/71 is produced large velocity variations of the range 0.664 to 0.696 m/sec, wafer/pad= 61/71 is obtained the velocity variation of range 0.667 to 0.693 m/sec and wafer/pad = 67/71 is observed the velocity variation of range 0.675 to 0.685 m/sec whereas at wafer/pad =71/71 is produced constant velocity distribution 0.679 m/sec. The observations show that the similar and reverse velocity profiles are obtained for the rpm ratios

73/71 and 79/71. In Fig. 5. the same process is repeated at the center to edge (r/R=1.0) of the wafer. The rpm ratio of the wafer/pad =59/71 is produced large velocity variations of the range 0.616 to 0.7437 m/sec, wafer/pad= 61/71 is obtained the velocity variation of range 0.627 to 0.733 m/sec and wafer/pad = 67/71 is observed the velocity variation of range 0.657 to 0.701 m/sec and the reverse velocity profile for the rpm ratios 73/71 and 79/71 are observed. In comparison, the high range of velocity variation is obtained at the edge of the wafer.

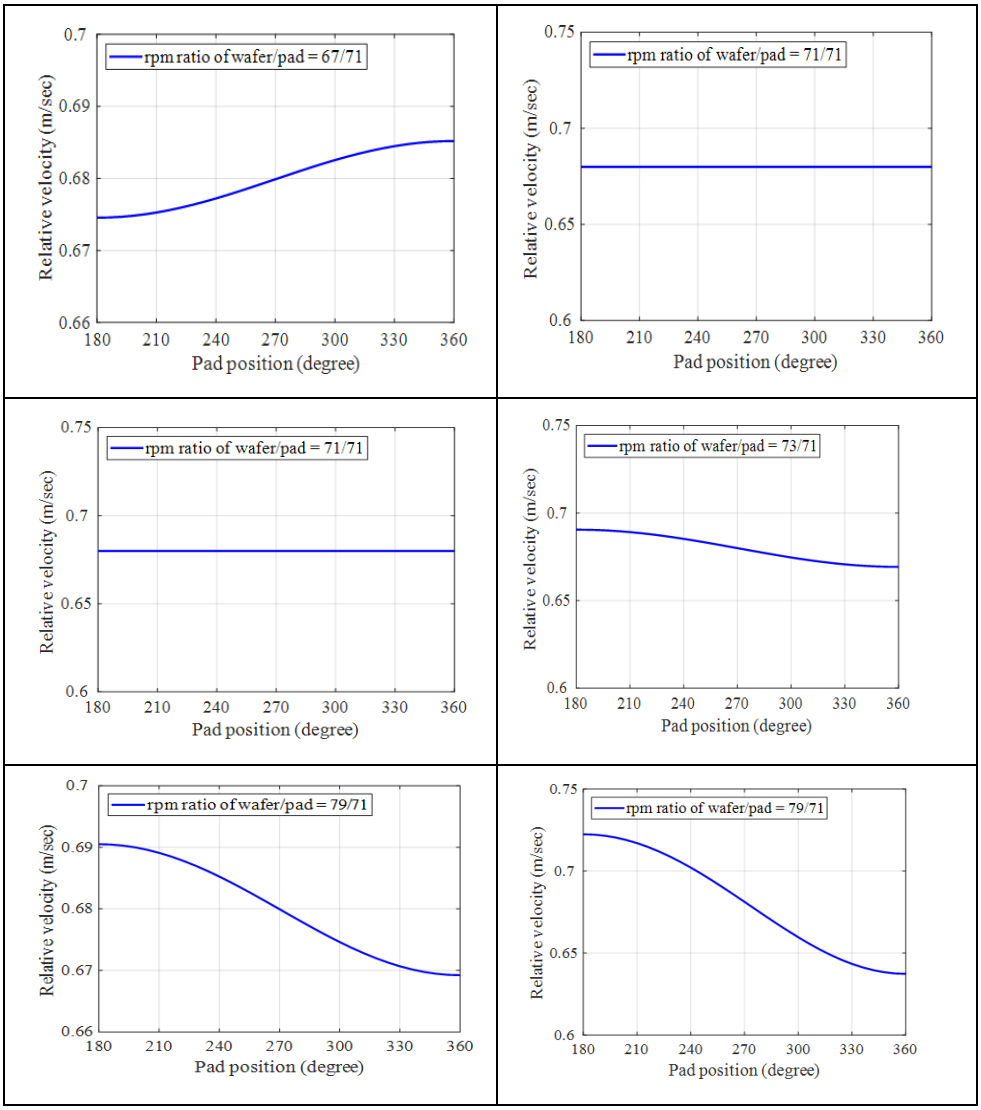

Figure 4. Velocity distribution at different rpm (r/R = 1.0 center to edge of wafer)

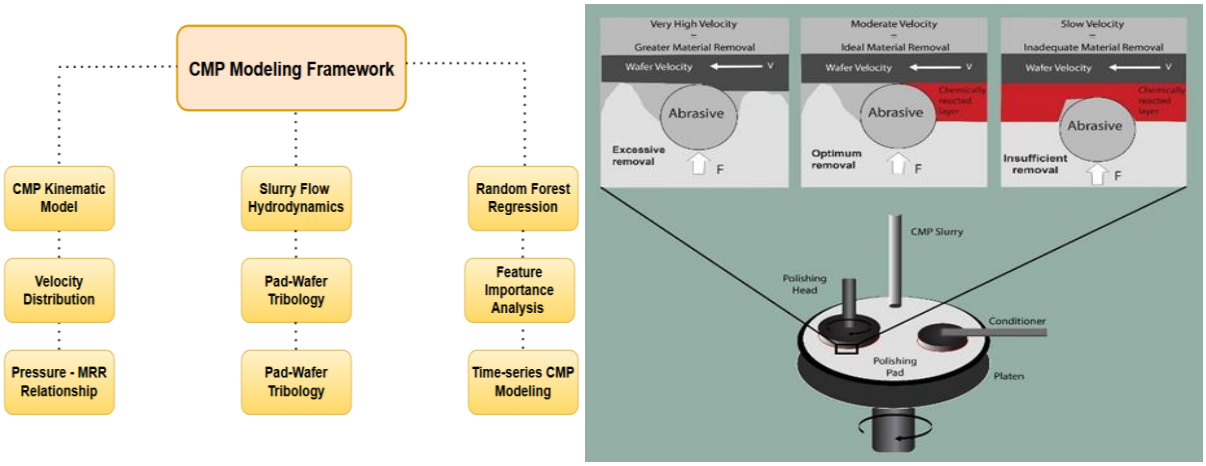

Figure 5. Effect of wafer rotational speed on velocity non-uniformity in CMP. The results show a decreasing trend in non-uniformity as wafer speed increases, highlighting the importance of speed optimization for uniform material removal.

The results shown in Fig. 8 show that the velocity non-uniformity dramatically decreases as the wafer rotating speed increases. Non-uniformity is comparatively high at lower wafer speeds (50–150 RPM), indicating uneven material removal over the wafer surface. The following is an elaboration of the figure results demonstrating that increasing wafer rotational speed resulted in a significant decrease in velocity non-uniformity: Higher velocity non-uniformity results from an uneven velocity distribution over the wafer at lower rotational speeds (50–150 RPM). Certain wafer sections are polished more or less vigorously as a result of this unevenness, which leads to uneven material removal rates. Local non-uniformities continue when the wafer speed is low because individual locations on the wafer surface do not move far enough to average the removal rate over time.

The wafer surface moves faster beneath the polishing pad as the rotating speed rises, which aids in averaging the impact of velocity variations throughout the wafer surface. By decreasing velocity non-uniformity, this enhanced motion improves overall wafer polish consistency and encourages a more uniform material removal rate.

2.2. Effect of Wafer Rotational Speed on Velocity Non-Uniformity in CMP

Fluctuations in interplanar distance (pm) and strain (%) throughout CMP wafer-pad layers under four conditions are depicted in Fig. 6. The interplanar distance generally decreases as the CMP layer number increases, indicating lattice contraction, while the strain fluctuates around zero percent, showing tensile or compressive strain changes dependent on the condition. Error bars show experimental consistency and variations by displaying variability for each measurement. For layered material systems, this image makes it easy to compare structural alterations and mechanical reactions between the four situations. These patterns provide insight into the effects of processing variables on mechanical integrity and crystal lattice relaxation, such as temperature, pad pressure, and polishing slurry chemistry. By balancing the tensile and compressive strains at crucial depths, an ideal CMP process will reduce the possibility of microcracking, delamination, or undesired electrical property changes. uniformity of material removal is influenced by the relative velocity distribution at the wafer-pad interface. This study examines the impact of wafer rotational speed on velocity non-uniformity to optimize polishing performance.

3. Results & Discussions

CMP process is mainly based on the material removal which is obtained by a complicated interaction between chemical and mechanical forces. The steady chemical reaction is generated the layer of the material between the wafer and slurry chemicals, which is removed by the mechanical abrasion with the sliding/rolling abrasives. Chemically-reacted film at the wafer surface is generated due to the oxidation/hydration process between the slurry chemical and wafer material.13 The notorious equation for the prediction of material removal rate (MRR) is the Preston equation, empirically established from the research of glass polishing processes in 1927.14 According to the Preston equation, the integral of the velocity along a period of time (t) is expressed the material removal rate.

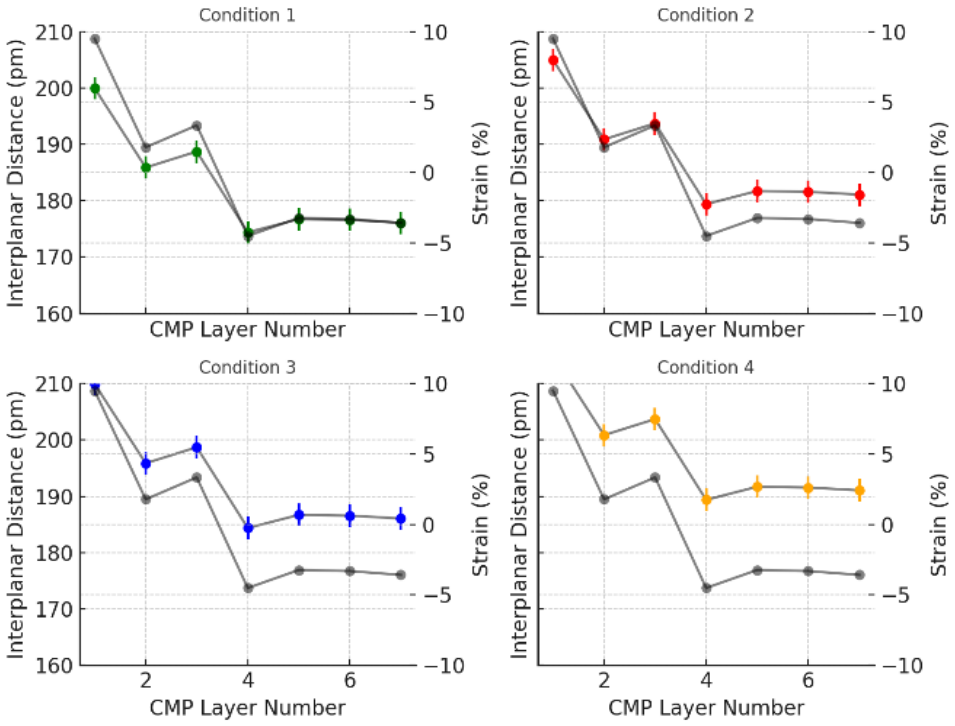

Figure 6. Variation in Interplanar Distance and Strain Among CMP Wafer-Pad Layers

$$MRR = \int_0^t k_p \,.\, P.\, V_{pad/wafer}\, dt \qquad (5)$$

where:

- **P** = Polishing pressure (downforce/pad-wafer contact area).
- $\mathbf{V_{pad/wafer}}$= Integral of the relative velocity at any point p on the pad surface with respect to wafer.
- **T**= polishing time.
- $\mathbf{k_p}$= Preston coefficient representing the effect of the other remaining parameters including the chemical reaction, pad property and so on.

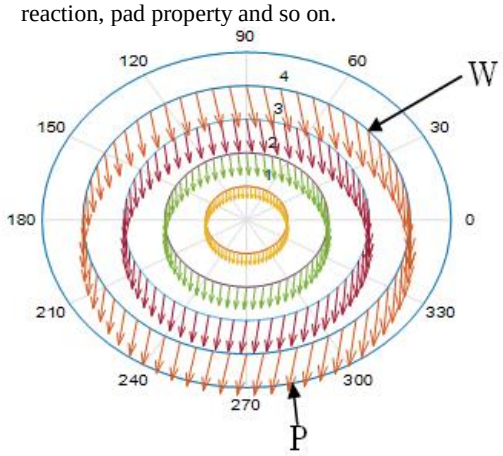

Figure 7. Velocity distribution for both pad/wafer motion with wafer = 59 rev/min and pad = 71 rev/min.

Fig. 7. is the vice versa vector plot as in Fig.2., which demonstrates the pad/wafer velocity distribution in terms of vector plot of four different radii at the wafer-pad interface with the wafer and pad rotational speeds are 59 rev/min and 71rev/min. On this basis, the material removal rate is elaborated as shown in Fig. 7. The defined rpm ratio of pad/wafer = 71/59showsthatthematerialremovalrateisthefunctionofpolishingtime for one revolution of the wafer. The result shows that the material removal rate is in the range of 0.94 to 1.14 nm/min during the polishing time of range 0 to 0.018 min in one revolution of wafer. Investigations of the material removal rate at different relative rotational speeds of pad/wafer for one revolution from the wafer edge are explained in table 1.Observations show that MRR decreases with the decrease of relative rpm ratios. For the MRR at the wafer edge from 59 to79 rpm is described in table 2. The results show that the MRR is in the range of 3.678 to 3.6712 nm/min.

Table 2. MRR at wafer edge

Pad/wafer rpm ratios	Time/rev. (min./rev)	Material Removed (nm)
71/59=1.2	0.01694	62.221
71/61=1.16	0.01639	60.027
71/67=1.059	0.0149	54.808
71/71=1.0	0.01408	51.708
71/73=0.973	0.01369	50.292
71/79=0.898	0.01265	46.511

Table 3. MRR at wafer edge from 50 to 79 rpm

Pad/wafer rpm ratios	MRR (microns/min)
71/59=1.2	3.678
71/61=1.16	3.677
71/67=1.059	3.672
71/71=1.0	3.6712
71/73=0.973	3.6713
71/79=0.898	3.674

Fig. 8. shows the MRR profiles from center to edge of the wafer. The observations show that the rpm ratio of pad/wafer = 71/59 is produced highest MRR of range 62.22 to 62.36 nm/min whereas the rpm ratio of pad/wafer = 71/79 is produced lowest MRR of range 46.465 to 46.515 nm/min among all the cases. The constant material removal rate around 51.7.

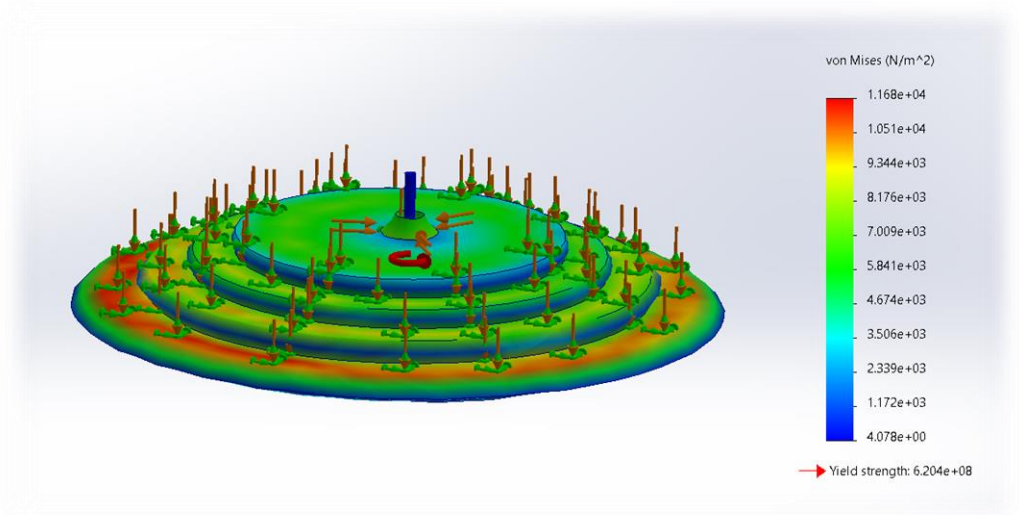

Figure 8. Von Mises stress isopleths detailing the structural mechanics of a Chemical Mechanical Planarization (CMP) platen, derived via sophisticated Finite Element Method (FEM) simulation.

3.1. MRR between pad-wafer rotation at varying polishing pressures:

It is observed that the removal rate increases as a function of the applied pressure. According to Eq. 5. the MRR between pad- wafer rotation developed the linear relationship with the polishing pressure. As the applied pressure is increased from 10.34 x 10-3 N/mm2 (10.34 kPa) to 20.34 x 10-3 N/mm2 (20.34 kPa), the removal rate is also increased.

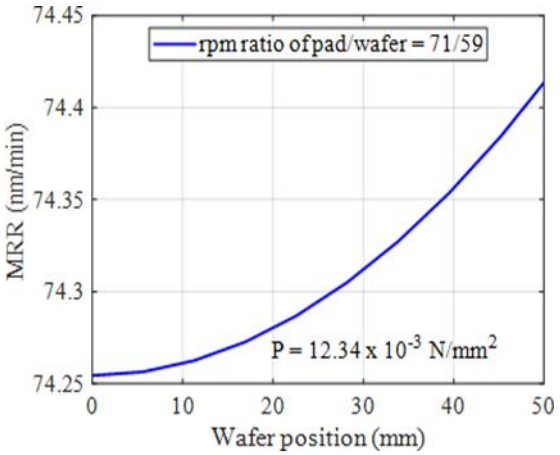

Figure 9. Material removal rate (MRR) as a function of polishing pressure with respect to wafer position from center to edge.

4. Comprehensive Analysis of Results

The material removal profiles that are displayed are deterministic expressions of the present hydro-mechanical non-idealities in rotary polishing equipment used in the production of high-fidelity semiconductors. The slurry film is not uniform. The rotation of the platen generates a hydrodynamic pressure field that is intrinsically non-symmetric relative to the wafer center. This pressure variation (often highest at the leading edge or specific radial positions) modulates the real contact area between the wafer and the pad asperities. The resulting pressure non-uniformity closely correlates with the observed tri-lobe removal profile. The mechanical anisotropy is effectively dampened by the Optimized Uniformity (71/59) condition, which reduces the difference between the maximum and minimum removed material.

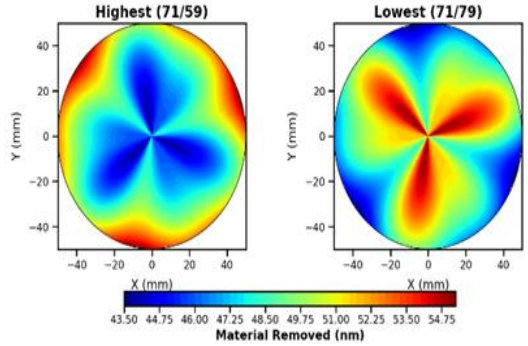

Figure 10. Spatial maps of material removal (nm) across the optic surface showing highest (71/59) and lowest (71/79) 3-lobe uniformity cases.

High-variance regions signify localized disturbances in the slurry flow or pad wear, which can impact the overall planarization efficiency. Identifying such inconsistencies is crucial for process optimization, as it allows for adjustments in pad conditioning, sweeping motion, or slurry distribution to enhance uniformity. The uniformity is also critically sensitive to how the pad is conditioned (roughened) by the diamond disc. The conditioning arm sweep path itself is often non-symmetric relative to the wafer's path.

5. Machine Learning-Based Prediction of Material Removal Rate in CMP

Conventional models, like Preston's equation make the assumption that process variables like relative velocity and polishing pressure and material removal rate (MRR) have a linear connection. Preston's equation is unable to account for the complex interactions introduced by elements like as slurry chemistry, pad wear, and rotational dynamics, which make CMP fundamentally non-linear.

5.1. Machine Learning Approach for Enhanced MRR Prediction

To address the limitations of traditional models, this study employs Machine Learning (ML) techniques to develop a more accurate predictive model for MRR. A Random Forest Regression model, known for its ability to capture non-linear relationships is trained using Leave-One-Out Cross- Validation (LOOCV) on experimental CMP data. This approach not only improves prediction accuracy but also provides feature importance analysis, offering deeper insights into the dominant factors affecting MRR in CMP.

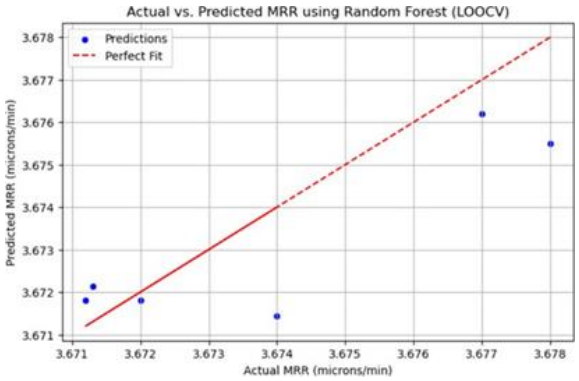

Figure 11. Actual vs. Predicted Material Removal Rate (MRR) using Random Forest with Leave-One-Out Cross-Validation (LOOCV).

5.2. Machine Learning Model: Random Forest Regression

To capture non-linear interactions between the parameters and MRR, a Random Forest Regression model was trained on the dataset. Given the small dataset size, Leave-One-Out Cross- Validation (LOOCV) was used instead of a standard train-test split to avoid issues related to sample scarcity. Hyperparameter Optimization: The model was fine-tuned using 100 decision trees (n_estimators=100).

5.3. Feature Importance Analysis

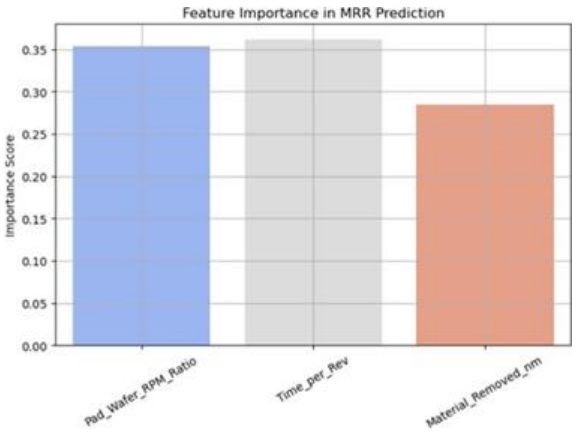

Figure 12. Feature importance in MRR prediction, showing the impact of Pad-Wafer RPM Ratio, Time per Revolution, and Material Removed (nm)

The feature importance analysis reveals which factors have the most significant impact on MRR prediction. This suggests that Pad/Wafer RPM Ratio is the dominant factor influencing MRR, followed by Material Removed (nm). The minor impact of Time per Revolution indicates that adjusting rotational speed is a more effective method for optimizing CMP performance.

5.4. Material Removal Rate and Slurry Flow Analysis in CMP using Machine Learning Techniques

This technique offers insights into process optimization by examining the link over time between pad velocity, downforce pressure, and slurry flow rate. We seek to comprehend the combined impact of these interdependent characteristics on the material removal rate (MRR) and surface finish uniformity. While changes in downforce pressure modify the mechanical abrasion intensity, variations in pad velocity directly affect the shear forces applied to the wafer surface. Furthermore, slurry flow rate is essential for preserving lubrication, uniformly dispersing abrasive particles, and avoiding excessive wear or localized overheating.

5.5. Multivariate Synergistic Topographical Deconstruction of CMP Wafer Pad Dynamics

The intricate interplay of mechanical abrasion, hydrodynamic slurry kinetics, and stochastic material removal phenomena in Chemical Mechanical Planarization (CMP) was systematically analyzed under controlled parametric variations. The work describes the spatiotemporal evolution of planarization efficacy using a dynamically controlled slurry flow regime, a wafer radius of 50 mm, and various pad/wafer rotational speed ratios (71/59, 71/61, 71/67, etc.). The relative velocity gradient (Vw/p), modulated within a normalized velocity distribution range of 0.375 to 1, and localized pressure fields (10.34 to 20.34 kPa) showed a considerable reliance on the material removal rate (3.671 to 3.678 μm/min). The anisotropic perturbations in material ablation are depicted by the emergent topographical heatmaps and 3D surface reconstructions, which also define areas of heightened wear and residual non-uniformities that are crucial for wafer surface convergence.

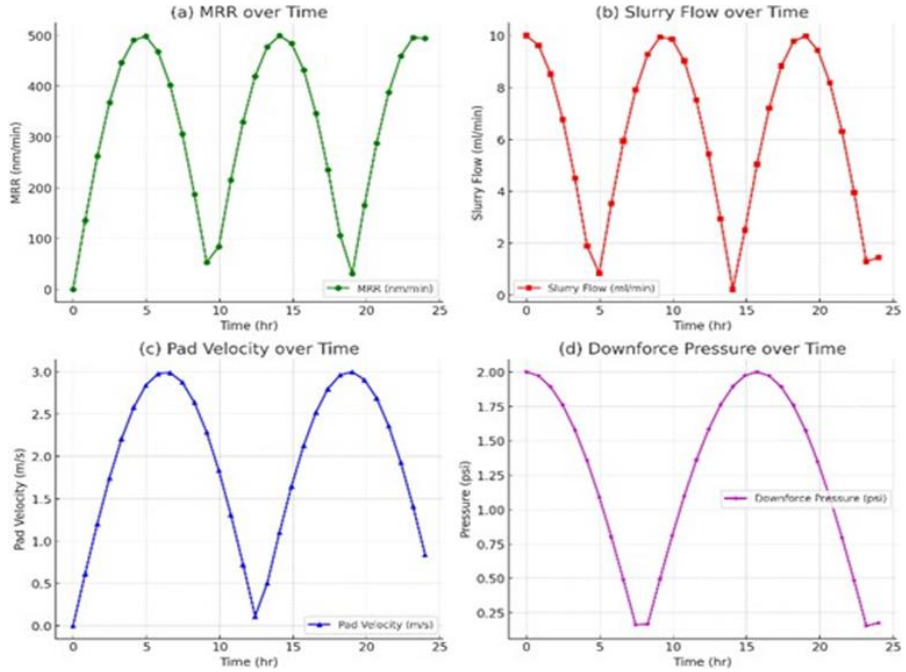

Figure 13. Time-based variation of key CMP parameters: (a) MRR (nm/min), (b) Slurry Flow (ml/min), (c) Pad Velocity (m/s), and (d) Downforce Pressure (psi). The trends indicate a strong interdependence between slurry distribution, pad dynamics, and material removal efficiency in the CMP process

A multi-scale, anisotropically resolved morphological breakdown of the topography of the CMP wafer pad is depicted in this picture, which integrates pressure-induced stochastic asperity attenuation, radial material removal stratification, and Gaussian-diffused planarization paths. Complex synergistic interactions between velocity-induced hydrodynamic transitions (normalized Vw/p: 0.375-1), pressure-modulated tribological constraints (10.34-20.34 kPa), and material removal kinetics (MRR: 3.671-3.678 μm/min) govern the reconstructed surface topology. These interactions all contribute to the emergent nonlinear wear profile seen across the wafer-pad interface. Pressure-dominated perimetric material reduction zones are revealed by a computationally generated radial gradient field, where planarization heterogeneity is exacerbated by localized asperity deformation. The competing interaction between slurry-induced shear stresses and contact-pressure- driven topographical evolution is highlighted by the simultaneous introduction of circumferential removal disparities caused by sinusoidal surface disturbances, which are varied by rotational pad/wafer RPM ratios (71/59, 71/61, 71/67, etc). Gaussian-smoothened asperity reconstructions of the resulting surface landscape show a spatially modulated topography induced by CMP, where the convergence or divergence of planarization uniformity in dynamically evolving CMP regimes is determined by rotationally driven shear force fluctuations, pressure-differentiated tribological wear fields, and hydrodynamically perturbed slurry transport.

5.6. Aberrant Kinetic Mechanisms of Sweeping Slurry Flow Dynamics in Chemical Mechanical Planarization (CMP) Under Rotational Perturbations:

The current study analyses the complex dynamics of the nitrogen 1s binding energy states under carefully regulated Fe- CN surface alterations, comparing atomic-scale reactivity changes with rotationally generated slurry-sweeping regimes. Using high-resolution X-ray Photoelectron Spectroscopy (XPS), the spectral deconvolution highlights the complex electron redistribution across defect-mediated interstitial domains, which is controlled by precisely adjusting the kinetics of the slurry-fluidic boundary layer. The inherent reliance of chemical state transitions on mechanical sweeping-induced surface renewal cycles is reflected in the spectral deconvolution across Fe-CN-modified surfaces under varied rotating fluidic stresses. At the wafer-pad interface, shear-driven slurry entrainment, load-induced dynamic adsorption, and turbulence- enhanced radical diffusion interact intricately to produce the observed peak shifts, intensity modulations, and spectrum widening. These findings offer a pioneering perspective on the atomic-scale response of wafer surfaces to dynamically evolving mechanical load conditions, paving the way for precision-engineered slurry formulations tailored to turbulence-optimized CMP efficiency.

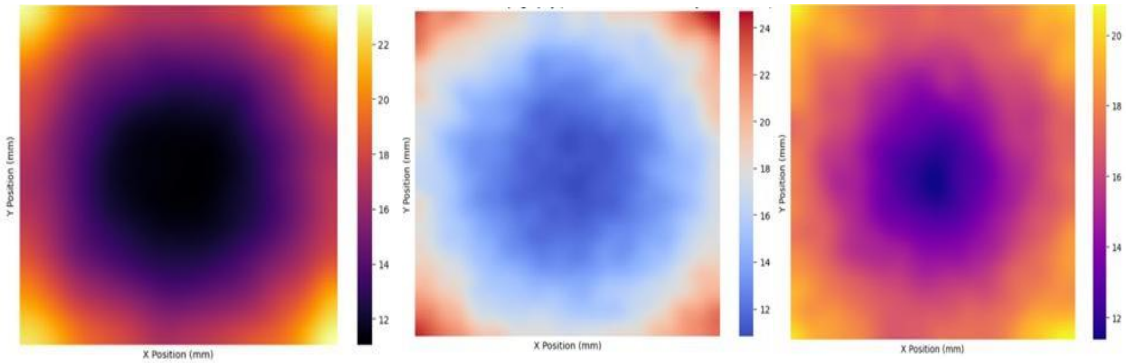

Figure 14. Computationally Augmented Stochastic Topographical Deconstruction of CMP Wafer Pad Surface Evolution Under Hydrodynamic Slurry Kinetics and Tribological Convergence

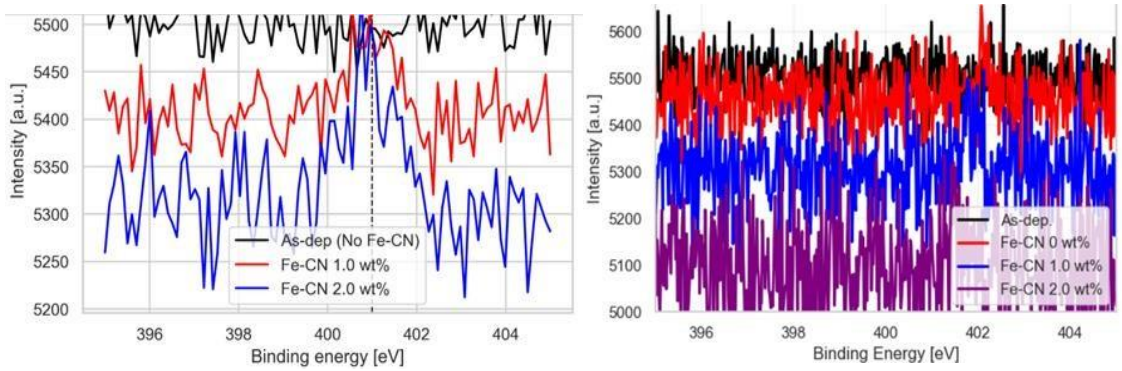

Figure 15. The complex interfacial electron redistribution phenomena resulting from rotationally regulated sweeping slurry flow in CMP are outlined by high-resolution XPS spectral deconvolution of N 1s binding states. The interaction of atomic-scale nitrogen coordination environments, dynamically reconstructed under multi-phase fluidic perturbations caused by sweeping rotational shear is demonstrated by the comparison spectra across different Fe-CN surface concentrations.

5.7. Parametric Evaluation of CMP Pad Wear Reduction via Novel Sweeping Kinematics in Conjugation with Preston's Model:

Comparing our kinematic sweeping model to traditional linear and uniform rotational dynamics the empirical results, shown in Fig. 20., clearly show a decrease in pad wear rates. This phenomenon's basic mechanism is the temporary redistribution of mechanical load vectors, which in turn reduces the localized stress concentrations that are usually the cause of excessive pad degradation. A statistically significant decline in material removal rates (MRR) were found by quantitative analysis, which was correlated with a nonlinear decrease in the Preston coefficient. These findings support our original hypothesis that without sacrificing planarization effectiveness, sweeping motion modifies the distribution of shear-induced stress fields, reducing pad deterioration and increasing operational lifespan. In order to maximize pad longevity and wafer uniformity, this study proposes a revolutionary change in CMP kinematics and the strategic application of dynamic rotational adjustments. These findings contribute to the advancement of next-generation CMP processes by providing a more efficient wear mitigation strategy, ultimately extending pad lifespan and improving planarization efficiency in wafer processing.

Conclusion

This work used kinematic modeling and machine learning-based prediction to examine the material removal rate (MRR) and velocity distribution in the CMP process. The assessed wafer-to-pad rotational speed ratios (59/71 to 79/71) demonstrated that MRR is directly impacted by velocity non-uniformity, which is lowest close to the wafer center and increases toward the edge. In line with Preston-based tendencies, greater RPM ratios resulted in larger MRR, while lower ratios decreased removal. Machine learning models further confirmed the dominant roles of Pad–Wafer RPM Ratio, Time per Revolution, and Material Removed (nm) in determining MRR, offering clearer insight into the nonlinear relationships governing CMP performance. These findings hold particular importance for advanced semiconductor manufacturers such as NVIDIA and TSMC, where extremely tight surface planarity is required for sub-5 nm logic, HBM stacking, and chiplet-based GPU/CPU architectures. Overall, the findings show that in the production of next-generation chips, data-driven parameter adjustment and improved kinematic control can greatly increase wafer uniformity, lower defectivity, and boost yield. To further increase dependability and manufacturability, future research should concentrate on sustainable CMP enhancements such lower slurry usage, longer-lasting pads, and improved edge-effect mitigation.

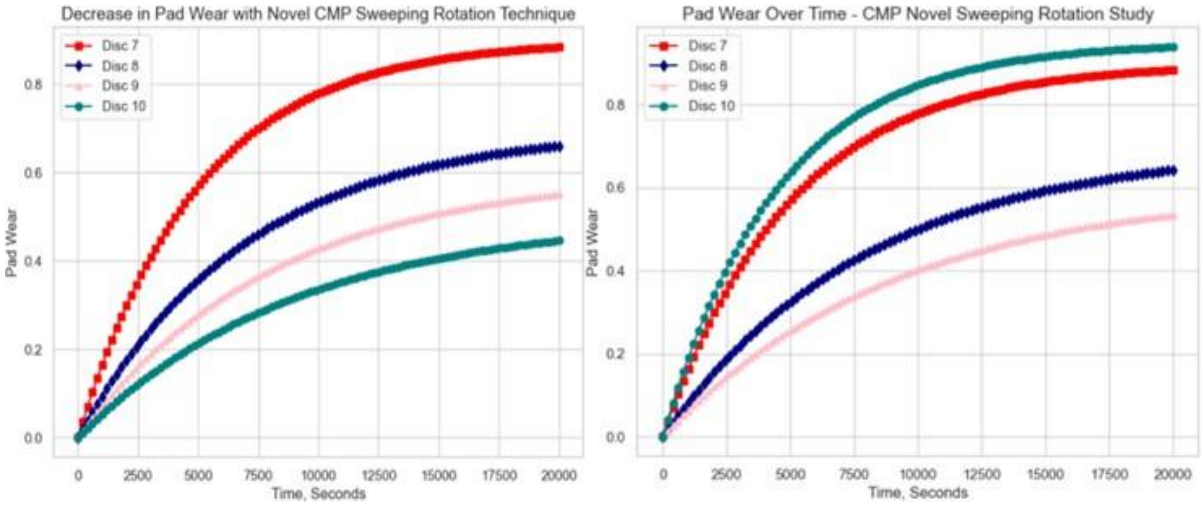

Figure 16. Experimental analysis of CMP pad wear reduction using the proposed sweeping kinematics model. The plotted data illustrate the effect of modified slurry flow dynamics and rotational sweeping motion on pad wear progression over time

References

[1] C. Rogers, J. Coppeta, L. Racz, A. Philipossian, and D. Bramono, “Analysis of flow between a wafer and pad during CMP processes”, Journal of Electronic Materials, Vol. 27, 1998, pp. 1082–1087. https://doi.org/10.1007/s11664-998-0141-0

[2] T. Tseng, J. Chin, and C. Kang, “Fundamentals of Slurry Design for CMP of Metal and Dielectric Materials”, Journal of the Electrochemical Society, Vol. 146, 1999, pp. 4191–4197. https://doi.org/10.1557/mrs2002.245

[3] H. Kim and H. Jeong, “Effect of process conditions on uniformity of velocity and wear distance of pad and wafer during chemical mechanical planarization”, Journal of Electronic Materials, Vol. 33, 2004, pp. 53–60. 10.1007/s11664-004-0294-4

[4] J. Yi, “On the wafer/pad friction of chemical-mechanical planarization (CMP) processes – Part I: Modeling and analysis”, IEEE Transactions on Semiconductor Manufacturing, Vol. 18, 2005, pp. 359–365.

[5] J. Yi, “Hydrodynamics of Slurry Flow in Chemical Mechanical Polishing: A Review”, IEEE Transactions on Semiconductor Manufacturing, Vol. 18, 2005, pp. 371–378.

[6] J. Terrell and F. Higgs III, “Broadband surface plasmon lasing in one-dimensional metallic gratings on semiconductor”, Journal of the Electrochemical Society, Vol. 153, 2006 https://doi.org/10.1038/s41598-017-08355-6

[7] H. Lee, D. Lee, and H. Jeong, “A review on chemical and mechanical phenomena at the wafer interface during chemical mechanical planarization”, International Journal of Precision Engineering and Manufacturing, Vol. 17, 2016, pp. 525–531.

[8] T. Feng, “Pressure and velocity dependence of the material removal rate in the fast-polishing process”, IEEE Transactions on Semiconductor Manufacturing, Vol. 20, 2007, pp. 451–458. https://doi.org/10.1364/AO.47.006236

[9] W. Yang, Y. Guo, Y. Li, and Q. Xu, “In-situ investigation of slurry flow fields during CMP”, Applied Optics, Vol. 47, 2008, pp. 6236–6243.

[10] Q. Ku, L. Chen, and J. Liu, “Effect of pH value and glycine in alkaline CMP slurry on the corrosion of aluminum by electrochemical analysis”, Journal of the Electrochemical Society, Vol. 156, 2009.

[11] Q. Xu, L. Chen, and H. Cao, “Pad-Wafer-Slurry Interface Information from Force Data”, ECS Journal of Solid-State Science and Technology, Vol. 8, 2019.

[12] Q. Xu, L. Chen, J. Liu, and H. Cao, “Slurry Supply Mechanism Utilizing Capillary Effect in Chemical Mechanical Planarization”, ECS Journal of Solid-State Science and Technology, Vol. 9, 2020. 10.1149/2.0111905jss

[18] Yun, S. Lee, and H. Kim, Re-examination of pressure and speed dependences of removal rate during chemical-mechanical polishing processes”, Journal of the Electrochemical Society, Vol. 18, 2023, pp. 1–10.

[13] Geroge Winkler, “Machine learning in chemical–mechanical planarization: A comprehensive review of trends, applications, and challenges”, International Conference on Mechanical Engineering and Automation Proceedings, 2025, pp. 1–7. https://doi.org/10.1016/j.aei.2025.103663

[14] T. Fujita and J. Watanabe, “Nano structuring methods for enhancing light absorption rate of Si-based photovoltaic devices: A review”, ECS Journal of Solid-State Science and Technology, Vol. 8, 2019, pp. P3069–P3076.

[15] F. Kaufman, D.Thompson, R. broadie, D.Pearson and M. Small, “Chemical-mechanical polishing for fabricating patterened W-metal features as chip interconnects”, Journal of the Electrochemical Society, Vol. 138, 1991, pp. 3460–3468.

[16] S. Hong, J. Bae, B. Koo, W. Cha, and B. Prinz, “Material removal rate model in chemical-mechanical polishing using micro-structured pads”, International Journal of Precision Engineering and Manufacturing – Green Technology, Vol. 1, 2014, pp. 67–75.

[17] J. Luo and D. Dornfeld, “Material Removal Mechanism in Chemical Mechanical Polishing: Theory and Modeling,” Proceedings of the International Conference on Chemical Mechanical Polishing Planarization, Santa Clara, USA, 2001